# YM155 as an inhibitor of cancer stemness simultaneously inhibits autophosphorylation of epidermal growth factor receptor and G9a-mediated stemness in lung cancer cells

Chun-Chia Cheng[1,2,3], Jungshan Chang[4], Stanley Ching-Cheng Huang[5], Huan-Chau Lin[1,2], Ai-Sheng Ho[6], Ken-Hong Lim[1,2], Chun-Chao Chang[7,8], Ling Huang[1,2], Yu-Cheng Chang[1,2], Yi-Fang Chang[1,2]*, Cheng-Wen Wu[3]*

1 Division of Hematology and Oncology, Department of Internal Medicine, MacKay Memorial Hospital, Taipei, Taiwan, 2 Laboratory of Good Clinical Research Center, Department of Medical Research, MacKay Memorial Hospital, Tamsui District, New Taipei City, Taiwan, 3 Institute of Clinical Medicine, National Yang-Ming University, Taipei, Taiwan, 4 Graduate Institute of Medical Sciences, School of Medicine, College of Medicine, Taipei Medical University, Taipei, Taiwan, 5 Department of Pathology & Immunology, Washington University School of Medicine, St. Louis, Missouri, United States of America, 6 Division of Gastroenterology, Cheng Hsin General Hospital, Taipei, Taiwan, 7 Division of Gastroenterology and Hepatology, Department of Internal Medicine, Taipei Medical University Hospital, Taipei, Taiwan, 8 Division of Gastroenterology and Hepatology, Department of Internal Medicine, School of Medicine, College of Medicine, Taipei Medical University, Taipei, Taiwan

* changyifang@gmail.com (YF Chang); ken@ibms.sinica.edu.tw (CW Wu)

## Abstract

Cancer stem cell survival is the leading factor for tumor recurrence after tumor-suppressive treatments. Therefore, specific and efficient inhibitors of cancer stemness must be discovered for reducing tumor recurrence. YM155 has been indicated to significantly reduce stemness-derived tumorsphere formation. However, the pharmaceutical mechanism of YM155 against cancer stemness is unclear. This study investigated the potential mechanism of YM155 against cancer stemness in lung cancer. Tumorspheres derived from epidermal growth factor receptor (EGFR)-mutant HCC827 and EGFR wild-type A549 cells expressing higher cancer stemness markers (*CD133*, *Oct4*, and *Nanog*) were used as cancer stemness models. We observed that EGFR autophosphorylation (Y1068) was higher in HCC827- and A549-derived tumorspheres than in parental cells; this autophosphorylation induced tumorsphere formation by activating G9a-mediated stemness. Notably, YM155 inhibited tumorsphere formation by blocking the autophosphorylation of EGFR and the EGFR-G9a-mediated stemness pathway. The chemical and genetic inhibition of EGFR and G9a revealed the significant role of the EGFR-G9a pathway in maintaining the cancer stemness property. In conclusion, this study not only revealed that EGFR could trigger tumorsphere formation by elevating G9a-mediated stemness but also demonstrated that YM155 could inhibit this formation by simultaneously blocking EGFR autophosphorylation and G9a activity, thus acting as a potent agent against lung cancer stemness.

## Introduction

The epidermal growth factor receptor (EGFR) overexpresses and activates the downstream phosphoinositide 3-kinase-AKT and mitogen-activated protein kinase-extracellular signal-regulated kinase (ERK; MEK) signaling pathways, respectively, thus regulating the survival and proliferation of cancer cells [1,2]. EGFR is particularly overexpressed in lung cancer. EGFR mutations have been reported to constitutively cause EGFR autophosphorylation [3,4]; the resulting poor patient survival rate is the major reason for drug resistance and tumor recurrence. EGFR overexpression exceeds 90% in lung cancer, acting as a target for potent therapeutic agents. Therefore, we hypothesized that EGFR participates in maintaining the cancer stemness property as the leading cause of tumor recurrence.

To test the hypothesis, we used YM155 to reduce tumorsphere formation derived from EGFR-positive lung cancer cells, because YM155 was demonstrated to suppress EGFR in pancreatic cells by degrading it [5]. We also investigated the detailed molecular mechanisms of YM155 as a potent inhibitor of cancer stemness cells (CSCs). YM155 was reported to be capable of reducing cancer stemness in gastric cancer [6]. In addition, the structure of YM155 is similar to that of a stemness inhibitor, BBI608 [7,8]. This evidence reveals that YM155 is a potent agent against lung cancer stemness. YM155 is an imidazolium-based survivin-suppressing compound that binds to interleukin enhancer-binding factor 3 (ILF3) [9] and inhibits a member of the inhibitor apoptosis protein [10]. Although YM155 inhibits anti-apoptosis by suppressing ILF3-mediated survivin, its detailed mechanism in the inhibition of cancer stemness is unclear.

In clinical practice, afatinib, a tyrosine kinase inhibitor (TKI), has been reported to inhibit EGFR phosphorylation and further suppress tumor progression [11–13]. Wang et al revealed that afatinib enhances the therapeutic efficacy of chemotherapeutic agents by suppressing CSCs [14]. Therefore, we proposed the hypothesis that the EGFR-mediated downstream pathway in the initiation of CSCs may be a target for discovering potent tumor therapeutic agents against cancer stemness. CSCs have been demonstrated to survive many tumor repressive treatments [15,16]. Post-translational modifications are critical for regulating the cellular function and phenotypic expression of cancer cells [17], thus leading to an immediate rescue of the cells under stressful therapeutic conditions. Furthermore, EGFR promotes chromatin condensation through methylation on H3K9 in KRAS-mutant lung A549 cells in response to stressful ionizing radiation [18]. Therefore, we proposed that the stemness property could be regulated by EGFR-mediated epigenetic modifications for maintaining the undifferentiating tumor status. Epigenetic modification enzymes, histone methyltransferases (HMTs) containing the SET domain, have been demonstrated to facilitate gene expression or silencing [19,20], thus possessing bivalent functions through methylation on histone 3 lysine residues. Among the HMTs, G9a, involved in embryonic development [21], was considered to maintain the stemness property in this study. G9a mainly methylates on histone 3 lysine 9 (H3K9) to regulate the transcriptional genes through gene silencing [22]. G9a can maintain CSC characteristics in head and neck squamous cell carcinoma [23]; therefore, we investigated whether G9a is generated as the downstream protein of EGFR in EGFR-positive lung tumor cells, for determining the stemness property in EGFR-positive lung cancer.

In this study, we established HCC827- and A549-derived CSC formation models and investigated the possible pharmaceutical mechanisms of YM155 against lung cancer stemness. We found that increased EGFR phosphorylation resulted in G9a upregulation in HCC827- and A549-derived tumorspheres to maintain cancer stemness. YM155 efficiently inhibited EGFR autophosphorylation and the EGFR-mediated G9a stemness pathway simultaneously, thus rendering it a potential agent against lung cancer stemness.

## Materials and methods

### Cell culture and tumorsphere formation

The lung cancer cell lines HCC827 and A549 were purchased from the American Type Culture Collection (ATCC, Manassas, VA, USA). The cell line H520 was purchased from Bioresource Collection and Research Center (BCRC, Hsinchu, Taiwan) and was authenticated through short tandem repeat profiling by BCRC; it was free of *Mycoplasma*. HCC827 and A549 were used for tumorsphere formation and Western blotting, and they were reauthenticated through short tandem repeat profiling (Applied Biosystems, Massachusetts, USA). The HCC827 and H520 cell lines were cultured in RPMI-1640 medium with 10% fetal bovine serum (FBS) and 1% penicillin–streptomycin. A549 was cultured in Dulbecco's modified Eagle medium (DMEM) with the same additives. For tumorsphere formation, the cells were cultured in low-attached 6-well plates with serum-free medium containing B27 (Invitrogen, Massachusetts, USA), 20 ng/mL of EGF (Sigma, Missouri, USA), 20 ng/mL of fibroblast growth factor (bFGF, Sigma), 5 μg/mL of bovine insulin (Sigma), and 4 μg/mL of heparin (Sigma) [24]. All cells were incubated at 37°C and 5% of $CO_2$. Cancer-initiating and early progenitor cells survived and proliferated, but differentiated cells died [25]. The cells were observed using an inverted microscope.

### mRNA extraction and cDNA preparation

The HCC827 cells and HCC827 CSCs were cultured in a 6-cm dish for mRNA extraction and harvested using 1 mL of TRIzol (Thermo Fisher Scientific, Massachusetts, USA). The solution was mixed with 200 μL of 1-bromo-3-chloropropane (Sigma), vortexed, and incubated for 5 min at room temperature. The supernatant was collected after 13,000-rpm centrifugation for 15 min at 4°C. Isopropanol (500 μL) was added and incubated for 5 min at room temperature. The pellet was collected after 13,000-rpm centrifugation for 10 min at 4°C. Subsequently, the pellet was incubated with 1 mL of 70% ethanol and centrifuged at 7500 rpm for 10 min at 4°C. Furthermore, the mRNA pellet was dissolved in double-distilled water after air drying. To obtain cDNA, 1 μg of mRNA, 2 μL of random hexamers, and 10 μL of double-distilled water were mixed in a polymerase chain reaction (PCR) tube and incubated at 65°C for 10 min, followed by cooling at 4°C. The solution was mixed with 4 μL of buffer (5×), 0.5 μL of RNase, 2 μL of dNTP (2.5 mM), and 0.5 μL of reverse transcriptase, and it was consequently treated at 25°C for 10 min, 50°C for 1 h, and 85°C for 5 min, followed by cooling at 4°C.

### Quantitative PCR

Quantitative PCR (Applied Biosystems, California, USA) was performed using the SYBR Green system (Applied Biosystems, California, USA) according to the manufacturer's instruction. The following primers were used. *Aldehyde dehydrogenase 1 (Aldh1)*: 5′–GTGGATTCAA GATGTCTGGAAATG–3′ and 5′–ATATTAGTGACTGTAAGGAGATGCT–3′. *CD133*: 5′– CTATTCAGGATATACTCTCAGCATT–3′ and 5′–TTTCTGTGGATGTAACTTTCAGTG–3′. *Oct4*: 5′–AAAGCAGAAACCCTCGT–3′ and 5′–TCCAGGTTGCCTCTCAC–3′. *Nanog*: 5′– GAGACAGAAATACCTCAGCC–3′ and 5′–TCTGCGTCACACCATTG–3′. *G9a*: 5′–GGGAG GAGCTAGGGTTTGAC–3′ and 5′–TGTGGTCCGTTCTCATGTGT–3′. *GLP*: 5′–CCAGTG CATGGCTACAGAGA–3′ and 5′–AGAAGTAGCCACAGCCAGGA–3′. *SUV39H1*: 5′–GGCAA CATCTCCCACTTTGT–3′ and 5′–CAATACGGACCCGCTTCTTA–3′. *SUV39H2*: 5′–GATTTA GAGGGCCCACCTTC–3′ and 5′–GGGAGTACCAGGTGGGATTT–3′. *SETDB1*: 5′–TCCCAG GATCTGCATAAAGG–3′ and 5′–TCAGCAGGAGGGTGGTAATC–3′. *SETDB2*: 5′–AGATG

TAACCAGGCGACCAC-3′ and 5′-TTCCTTCTTTTGTGGCATCC-3′. *GAPDH*: 5′-GAGT
CAACGGATTTGGTCGT-3′ and 5′-TTGATTTTGGAGGGATCTCG-3′.

## Gene knockdown

*EGFR* and *G9a* knockdown was conducted using a short-hairpin RNA (shRNA)-expression
lentivirus system that contains the specific shRNA in the vector pLKO.1-puro generated in
293T cells. The *EGFR* and *G9a* pLKO plasmid and scrambled control were purchased from
National RNAi Core Facility of Academia Sinica, Taipei, Taiwan. For producing lentivirus,
293T cells (70% confluence) cultured in DMEM containing 10% FBS and 0.1% penicillin–
streptomycin (6-cm dish) were transfected with 4 μg of *EGFR* or *G9a* pLKO.1 vectors, 1 μg of
the envelope plasmid pVSV-G, and 3.6 μg of the packaging plasmid pCMVΔR8.91. The plas-
mids were preincubated with 400 μL of Lipofectamine 2000 for 20 min at room temperature
and consequently added to 293T cells. The cultured medium was substituted with fresh
DMEM containing 30% FBS and 1% of penicillin–streptomycin and incubated for 4 h. The
virus solution was collected after 48 h of transfection and stored at −80˚C. HCC827 or A549
cells cultured in 80% confluence were infected with the prepared lentivirus (preincubated with
8 μg/mL of polybrene) for 24 h. The cells were then changed with RPMI-1640 medium for
HCC827 cells or DMEM for A549 cells containing 10% FBS, 1% penicillin–streptomycin, and
2 μg/mL of puromycin, which were harvested after 48 h.

## Western blotting

The cells were lysed in RIPA buffer containing 50 mM Tris-HCl (pH 7.4), 1% NP-40, 0.5%
Na-deoxycholate, 0.1% sodium dodecyl sulfate (SDS), 2 mM ethylenediaminetetraacetic acid,
50 mM NaF, and 150 mM NaCl. The lysed proteins were mixed with 5× sample buffer [75 mM
Tris-HCl, pH 6.8, 10% (v/v) glycerol, 2% SDS (w/v), 0.002% (w/v) bromophenol blue]. In
total, 20 μg of each sample was analyzed through 10% SDS-polyacrylamide gel electrophoresis
and then transferred onto Immobilon-P polyvinylidene fluoride (PVDF) membranes (Merck
Millipore, Massachusetts, USA). These membranes were blocked with 5% skim milk for 1 h at
room temperature, incubated with primary antibodies (1 μg/mL) overnight at 4˚C, and
washed using Tris-buffered saline with 0.1% Tween-20. The specific antibodies against EGFR,
pEGFR (Y1068), and mH3K9 were purchased from Cell Signaling (Danvers, Massachusetts,
USA), and Oct4 and G9a were purchased from Novus Biologicals (Littleton, Colorado, USA).
After washing, the PVDF membranes were incubated with horseradish peroxidase-conjugated
secondary antibody (1 μg/mL) for 2 h at room temperature. The immunoreactive proteins
were detected through an enhanced chemiluminescence kit (Bio-Rad, California, USA) cou-
pled with an LAS-4000 mini device (Fujifilm, Tokyo, Japan).

## Cell viability

The WST-1 (2-(4-iodophenyl)-3-(4-nitrophenyl)-5-(2,4-disulfophenyl)-2H-tetrazolium,
monosodium salt; Takara) assay was used to determine cell viability after incubation with
YM155, afatinib, and UNC0642 for 48 h. At least three replicates were performed.

## Statistical analysis

Statistical analyses were performed using GraphPad Prism V5.01 (GraphPad Software, Inc.,
California, USA). All analytical data with more than two groups were evaluated using analysis
of variance, followed by post hoc analysis with Bonferroni's test. Student's t test was used to

compare two groups. Moreover, $p < 0.05$ was considered to indicate a statistically significant difference.

## Results

### Elevated autophosphorylation (Y1068) of EGFR and methylation on H3K9 in HCC827-formed tumorspheres

To investigate the molecular mechanism of CSCs in EGFR-positive lung cancer, we first examined the expression of EGFR in three lung cancer cell lines, namely HCC827, A549, and H520. HCC827 (EGFR E746-A750 deletion) and A549 (EGFR wild-type) are adenocarcinomas, whereas H520, an EGFR-negative cell line, is a squamous carcinoma of the lung (Fig 1A). Western blotting revealed higher EGFR expression and autophosphorylation in HCC827 cells than in A549 and H520 cells (Fig 1A). HCC827 cells were adherent but could form a tumorsphere exceeding 100 μm in 12 days (Fig 1B) when cultured in a low-attached dish with serum-free medium, as described in the Materials and Methods section. A549 (EGFR-positive) and H520 (EGFR-negative) cells could also form tumorspheres in 7 days in the addition of 4 growth factors, EGF, FGF, insulin, and heparin (Fig 1C), whereas, EGF only triggered A549 to form tumorspheres (Fig 1C). We further identified the stemness characteristics in the formed tumorspheres through quantitative reverse transcription PCR by measuring the expression of cancer stemness markers, namely *Aldh1*, *Cd133*, *Oct4*, and *Nanog*. The results indicated higher expression levels of *Aldh1*, *Cd133*, *Oct4*, and *Nanog* in the tumorspheres (HCC827 CSCs) than in parental HCC827 cells (Fig 1D). Moreover, A549 CSCs expressed higher mRNA levels of *Cd133*, *Oct4*, and *Nanog* but exhibited reduced mRNA levels of *Aldh1* (Fig 1E). Both stemness models were used to investigate the cellular stemness property of EGFR-positive lung cancer. We subsequently investigated the growth factors (EGF, FGF, insulin, and heparin in the FBS-free B27-supplement medium) that majorly regulate the formation of HCC827 tumorspheres. We cultured HCC827 cells in the medium without EGF, FGF, insulin, or heparin and investigated tumorsphere formation. Notably, HCC827 formed tumorspheres even in the absence of growth factors in the culture (Fig 1F). In addition, we cultured HCC827 cells in the FBS-free B27-supplement medium without growth factors and determined the phosphorylation of EGFR on Y1068 through Western blotting. According to our review of the relevant literature, the autophosphorylation of EGFR on Y1068 can lead to the activation of the granzyme B 2-RAS-RAF-MEK1-ERKs and Janus activated kinase-signal transducer and activator of transcription 3 pathways [26]. Moreover, pY1068 was suggested to be a predictive biomarker for EGFR-TKI treatment [27]. Therefore, this phosphorylated site on Y1068 of EGFR was determined for representing the activation of EGFR. The phosphorylation of EGFR was increased in HCC827 cells cultured in the serum-free medium without growth factors (Fig 1G), suggesting that EGFR activation was the temporary cellular response to the environmental stress under a serum-free condition, which may result in tumorsphere formation. In addition, the HCC827-derived tumorspheres presented higher levels of EGFR phosphorylation, methylation on H3K9, and Oct4 expression than did parental HCC827 cells (Fig 1D), whereas Oct4 was used as a stemness marker.

### YM155 significantly blocked the formation of tumorspheres and inhibited phosphorylation of EGFR and expression and activity of G9a

To elucidate and investigate the possible mechanism of the stemness property in EGFR-positive lung cancer, we used YM155, a stemness inhibitor, and investigated its cellular mechanism and potential as an inhibitor of cancer stemness in EGFR-derived cancer stemness models.
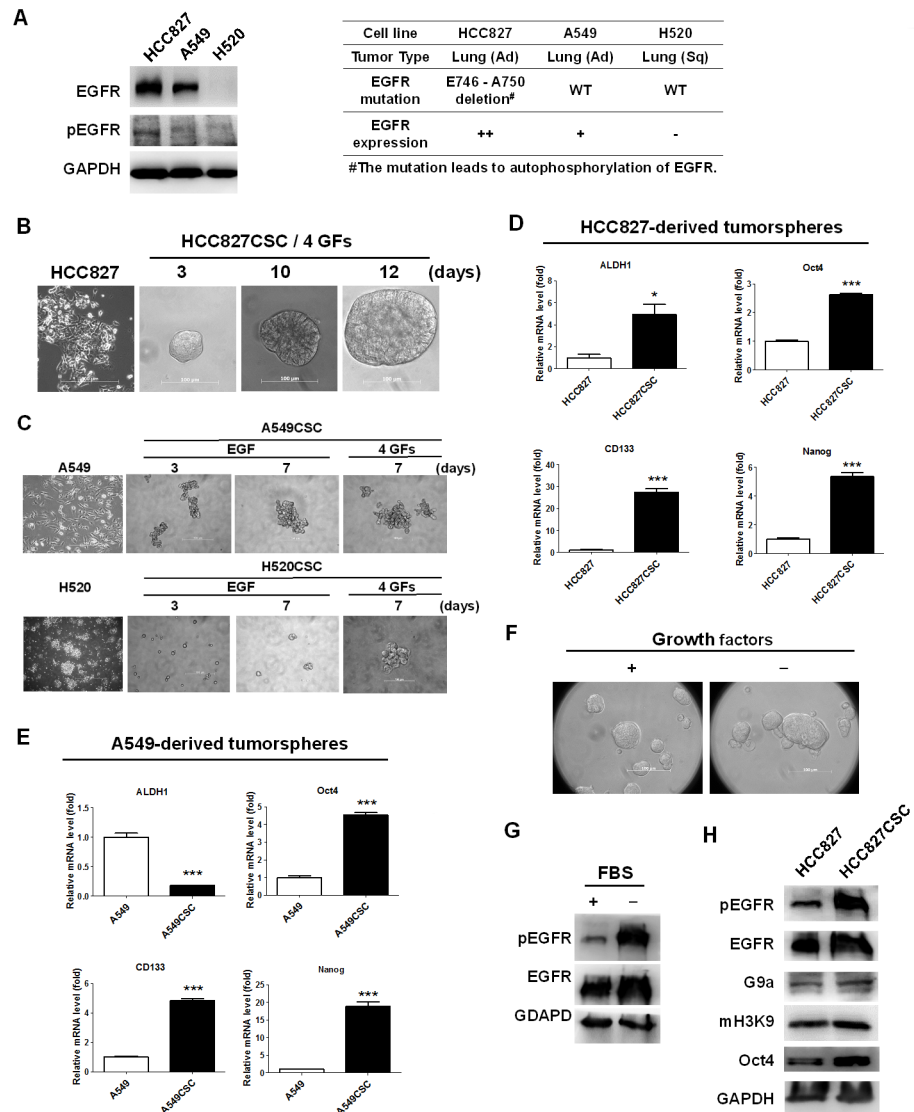
**Fig 1. Elevated phosphorylation of EGFR and G9a-mediated methylation on H3K9 in HCC827-derived CSCs.** (A) HCC827^{++}, A549[+], and H520[−] were selected for analyzing EGFR phosphorylation. (++) high expression; (+) moderate expression; (−) no expression. The results indicated higher EGFR expression in HCC827 cells than in A549 and H520 cells, whereas autophosphorylation of EGFR in HCC827 cells. (B and C) HCC827- or A549-derived tumorspheres were detected and imaged through inverted microscopy when the cells were cultured in a low attached dish with FBS-free B27 supplement medium. For triggering the formation of temporary CSCs, four additive growth factors (4 GFs) were added, namely EGF, bFGF, insulin, and heparin. (D) HCC827- and A549-derived tumorspheres were investigated to detect the expression of stemness markers, *ALDH1*, *CD133*, *Oct4*, and *Nanog*, for identifying the stemness property. These markers were increased in HCC827 CSCs (n = 3) compared with parental HCC827 cells (n = 3), but (E) only *CD133*, *Oct4*, and *Nanog* were increased in A549 CSCs. (F) In addition, HCC827 cells cultured in serum-free B27 supplement medium without the aforementioned factors formed tumorspheres with (G) elevated EGFR phosphorylation. (H) EGFR phosphorylation was higher in HCC827 CSCs than in parental HCC827 cells, accompanied by higher G9a expression and H3K9 methylation, whereas *Oct4* was used as a stemness marker. Scale bar: 100 μm. *$p < 0.05$ and ***$p < 0.001$.

YM155 was treated with HCC827 and A549 cells in a dose-dependent manner for investigating its cytotoxic capacity in parental lung cancer cells. The results revealed that more than 100 ng/mL of YM155 could reduce the viability of HCC827 cells (Fig 2A). Moreover, 1 ng/mL of YM155 was more sensitive to A549 cells and led to similar inhibition in cell viability compared with HCC827 cells (Fig 2B). Furthermore, 10 ng/mL of YM155 markedly reduced the size of HCC827-derived tumorspheres and resulted in lower cell viability (Fig 2C), in addition to inhibiting A549-derived tumorsphere formation (Fig 2D). Considering the inhibitory activity of YM155 in parental HCC827 and A549 cells, YM155 seemed to perfer to inhibit the growth of tumorspheres owing to its higher capacity to inhibit the viability of tumorspheres at 10 ng/mL.

We found that YM155 inhibited the autophosphorylation of EGFR in HCC827 (Fig 2E) and A549 (Fig 2F) CSCs, resulting in the reduction in *Oct4* expression. Afatinib was used as a positive control to inhibit the phosphorylation of EGFR, which also resulted in the reduction in *Oct4* expression in HCC827 CSCs (Fig 2E). Next, to explore the EGFR-downstream regulators involved in the cancer stemness property, we investigated whether SET domain-containing proteins, which can methylate on H3K9, were associated with maintaining this property. We measured the expression of the SET domain-containing proteins *SUV39H1*, *SUV39H2*, *G9a*, *GLP*, *SETDB1*, and *SETDB2*. The results revealed that the expression levels of *SUV39H2*, *G9a*, *GLP*, and *SETDB2* were significantly increased in HCC827 CSCs compared with parental HCC827 cells (Fig 2G). In addition, YM155 treatment reduced *G9a* and *GLP* expression (Fig 2H), implying that YM155 regulates *G9a* and *GLP* expression in HCC827 CSCs.

In clinical practice, *G9a* mRNA levels were associated with a poor survival rate in lung adenocarcinoma ($p = 0.0011$), as analyzed using the MatInspector program based on The Cancer Genome Atlas (TCGA) database (Fig 2I) [28]. This result indicates that *G9a* is oncogene among *SUV39H2*, *GLP*, *and SETDB2*. We then investigated whether EGFR could regulate *G9a* expression and explored the regulatory effects of YM155 in EGFR-positive HCC827 cells co-treated with EGF. We observed that YM155 reduced the autophosphorylation of EGFR and the expression and activity of G9a in HCC827 cells (Fig 2J), accompanied by reduced *Oct4* expression (Fig 2J). However, YM155 did not inhibit the autophosphorylation of EGFR in EGF co-treatment cells (Fig 2J). A549 cells were subsequently used for investigating the EGFR-G9a regulatory pathway. We treated A549 cells with 20 ng/mL of EGF in a time-dependent manner. The results revealed that EGF induced EGFR phosphorylation in 0.5 h, consequently resulting in the expression of G9a and Oct4, whereas H3K9 methylation served as an activation marker of G9a (Fig 2K).

## Inhibition of EGFR reduced expression and activity of G9a and HCC827-derived tumorsphere formation

EGFR phosphorylation was higher in HCC827-derived tumorspheres and EGF induced the expression of G9a and Oct4, implying that EGFR participated in tumorsphere formation. Therefore, to evaluate whether EGFR plays a pivotal role in tumorsphere formation, we blocked EGFR phosphorylation using afatinib. Afatinib was treated with or without EGF in HCC827 cells. We observed that 20 ng/mL of EGF induced the expression of *G9a* and *Oct4* in HCC827 cells (Fig 3A), which was suppressed by afatinib (Fig 3A). Compared with YM155, afatinib inhibited the phosphorylation of EGFR in EGF co-treated cells, resulting in a marked reduction of the methylation on H3K9 (Figs 2I and 3A). To specifically ensure that the expression and activity of *G9a* are regulated through EGFR phosphorylation, EGFR was targeted with a knocked down shRNA, which markedly reduced the expression of EGFR, *Oct4*, *G9a*,
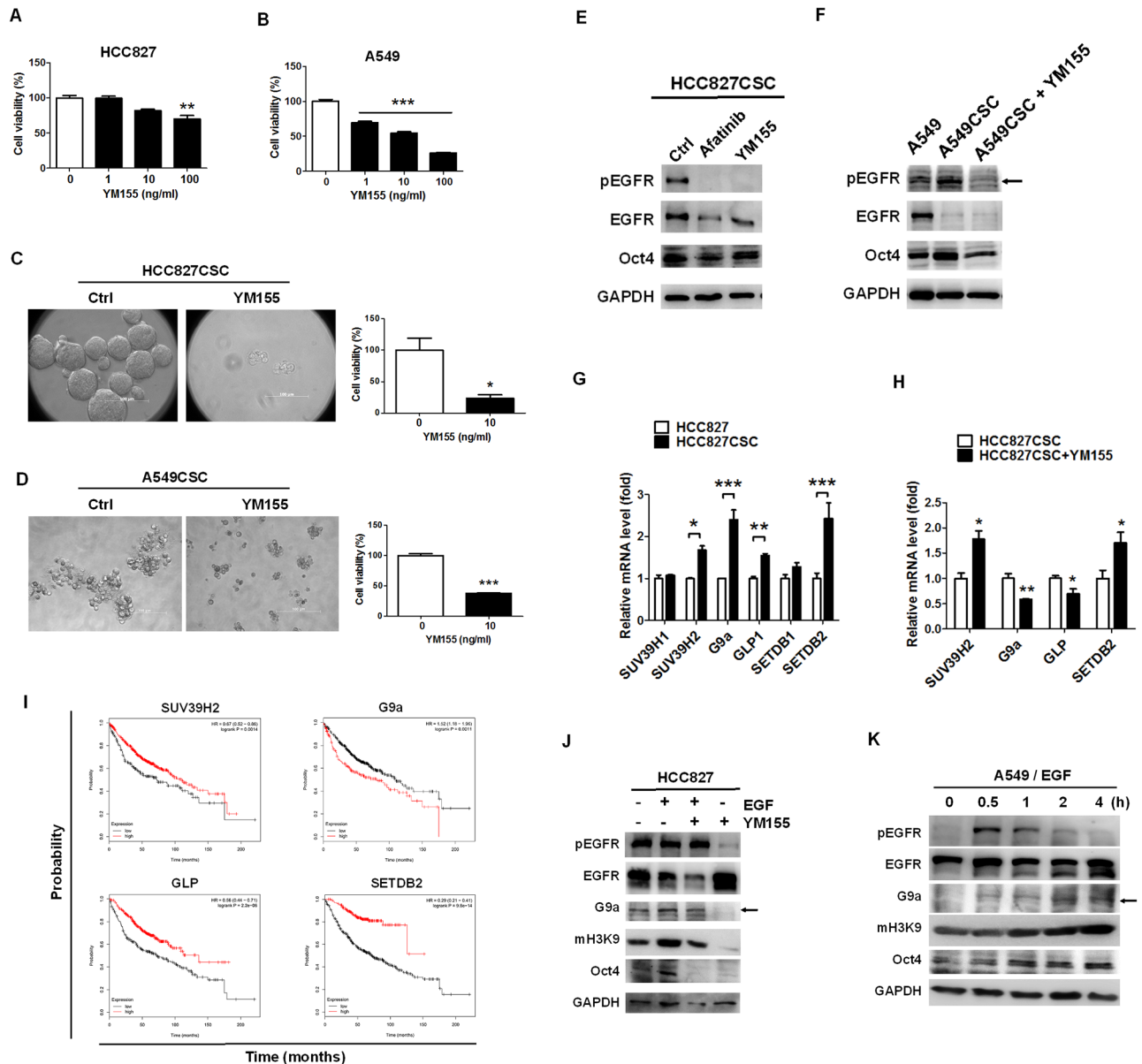
**Fig 2. YM155 significantly reduced tumorsphere formation and inhibited EGFR autophosphorylation and G9a expression.** YM155 is reported to suppress cancer stemness; therefore, we used this compound to investigate the cellular mechanism of tumorsphere formation. To compare the cytotoxic capacity of YM155 against tumorsphere formation and parental cell lines, YM155 was applied to HCC827 and A549 cells in the stemness cultured or integrated medium. (A) YM155 significantly reduced HCC827 cells when used at a dose of 100 ng/mL ($**p < 0.01$) and (B) A549 cells when used at a dose of 1 ng/mL ($***p < 0.001$). (C) Microscopy revealed that 10 ng/mL of YM155 considerably inhibited the formation of HCC827 and (D) A549CSC tumorspheres and resulted in a lower cell viability. (E) Because EGFR overexpresses in HCC827 and A549 cells, and because YM155 has been reported to suppress EGFR, we investigated the autophosphorylation status of EGFR in HCC827- and A549-derived tumorspheres. EGFR phosphorylation was blocked by YM155 in HCC827-derived tumorspheres, whereas afatinib, a tyrosine kinase inhibitor, was used as a control. (F) Moreover, YM155 inhibited EGFR autophosphorylation in A549-derived tumorspheres and reduced *Oct4* expression. (G) The methylation on H3K9 was high in HCC827-derived tumorspheres; therefore, we investigated the mRNA levels of the SET domain-containing proteins, particularly those functioning in H3K9 methylation, in HCC827 CSCs compared with parental HCC827 cells. The results revealed that the mRNA of *SUV39H2*, *G9a*, *GLP*, and *SETDB2* increased in HCC827 CSCs. (H) In addition, YM155 significantly reduced the mRNA levels of *G9a* and *GLP* but increased those of *SUV39H2* and *SETDB2*. (I) To confirm the significant roles of tumorsphere-expressed *SUV39H2*, *G9a*, *GLP*, and *SETDB2* in lung adenocarcinoma, the Kaplan–Meier method was used for investigating the relationship between the mRNA levels of *SUV39H2*, *G9a*, *GLP*, and *SETDB2* and the survival rate in 2,437 patients with lung cancer; the mean follow-up period was 49 months. The results revealed that an elevated mRNA level of *G9a* was associated with a lower overall survival rate in the patients with lung adenocarcinoma, but the remaining three genes yielded controversial results. Higher gene expression levels are indicated in red. (J) We

investigated whether EGFR could downregulate *G9a* expression in HCC827 cells. We found that YM155 reduced EGF-induced *G9a* expression, H3K9 methylation, and *Oct4* expression in HCC827 cells. HCC827 cells were treated with 20 ng/mL of EGF with or without 10 ng/mL of YM155. (K) HCC827, an EGFR-mutant strain, can induce autophosphorylation; therefore, we investigated and validated EGFR-regulated *G9a* expression in EGFR wild-type A549 cells. A549 cells treated with 20 ng/mL of EGF expressed immediate EGFR autophosphorylation in 0.5 h and subsequent *G9a*, mH3K9, and *Oct4* expression. The results indicated that EGF induced the expression of *G9a* and *Oct4* in lung cancer. Scale bar: 100 μm. *$p < 0.05$.

and *mH3K9* (Fig 3B); this suggests that EGFR regulates the expression and activity of G9a and maintains the stemness property in lung HCC827 cells.

Next, afatinib significantly inhibited the viability of HCC827 cells in a dose-dependent manner (Fig 3C), and it also reduced tumorsphere formation at a dose of 10 ng/mL (Fig 3D), leading to an approximately 50% reduction in cell viability, similar to the effects of afatinib on parental HCC827 cells (Fig 3C and 3D). To ensure that the tumorsphere reduction was engendered from the inhibition of the stemness property, afatinib-treated tumorspheres were collected and analyzed through Western blotting for measuring *Oct4* expression. We observed that afatinib blocked EGFR autophosphorylation and also reduced *Oct4* expression in HCC827 CSCs (Fig 3E).

## G9a determined EGFR-mediated stemness in lung cancer cells

To understand the role of G9a in tumorsphere formation, we treated HCC827 and A549 cells with UNC0642, an inhibitor antagonizing *G9a* and *GLP* [29]. We observed that UNC0642 markedly reduced the viability of the cells in a dose-dependent manner (Fig 4A and 4B). Moreover, UNC0642 reduced tumorsphere formation in HCC827- and A549 CSCs (Fig 4C and 4D), with a significant reduction in viability at a dose of 10 μg/mL; the results indicate that G9a plays an important role as the downstream protein in the cancer stemness activity. Furthermore, to validate that G9a regulates the stemness property in lung cancer and understand whether it downregulates EGFR signaling in lung cancer cells, UNC0642 was co-treated with or without EGF in HCC827 cells. We found that UNC0642 reduced G9a activity, as indicated by the expression of mH3K9, and inhibited EGF-induced *Oct4* expression (Fig 4E). In addition, we knocked down G9a by using a specific shRNA technique in A549 cells and found that G9a reduction resulted in the downregulation of mH3K9 and *Oct4* (Fig 4F). *G9a* knockdown, as confirmed by measuring the mRNA levels (Fig 4G), resulted in the reduction in the mRNA levels of *CD133* (Fig 4H), *Oct4* (Fig 4I), and *Nanog* (Fig 4J), suggesting that G9a determined the cancer stemness property in A549 cells. These results reveal that YM155 reduced tumorsphere formation by inhibiting the EGFR-mediated activation of *G9a* in the cancer initiation program of HCC827 and A549 CSCs.

## Discussion

CSCs are the main reason for tumor recurrence. In this study, we demonstrated that EGFR triggered the formation of tumorspheres derived from HCC827 and A549 cells, which expressed *CD133*, *Oct4*, and *Nanog* used as the cancer stemness models. We observed that the potential EGFR-G9a pathway played an essential role in the formation of lung CSCs. This study also revealed that YM155 simultaneously inhibited the autophosphorylation of EGFR and G9a-mediated stemness property in HCC827 and A549 cells, thus rendering it an efficient anti-stemness inhibitor.

According to our review of the relevant literature, EGFR overexpression exceeds 90% in lung cancer. Therefore, targeting EGFR is considered an efficient therapeutic strategy against
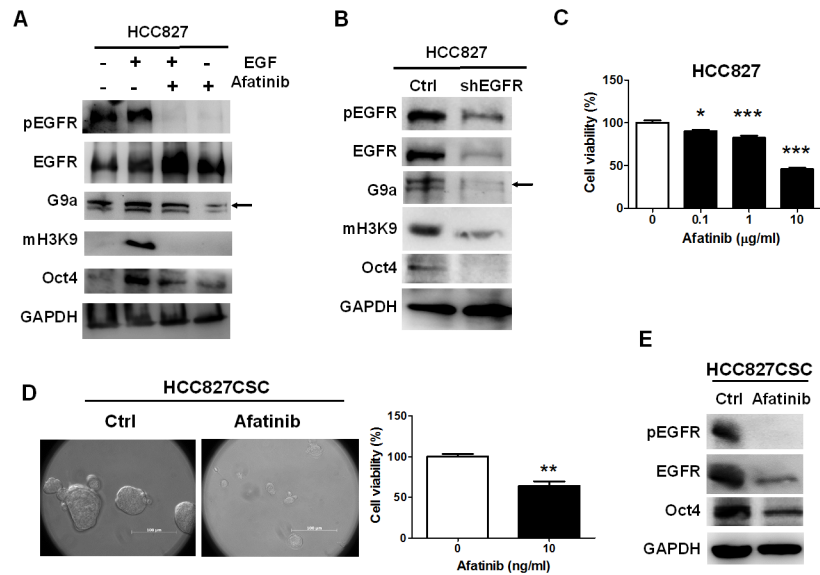
**Fig 3. EGFR induced the formation of HCC827-derived tumorspheres and *G9a* expression.** To validate that EGFR directly affects the expression of *G9a* and *Oct4* involved in tumorsphere formation, we inhibited EGFR by using afatinib and genetic knockdown to demonstrate the EGFR-G9a regulatory relationship. (A) Afatinib treatment with or without 20 ng/mL of EGF blocked *G9a* expression and H3K9 methylation, accompanied by the reduction in *Oct4* expression, indicating that EGFR positively regulated *G9a* in HCC827 cells. (B) EGFR knockdown with lower EGFR autophosphorylation also reduced *G9a* expression, H3K9 methylation, and *Oct4* expression. (C) To validate whether the blockade of EGFR phosphorylation can reduce tumorsphere formation, afatinib was used. First, afatinib was treated with parental HCC827 cells at a dose of more than 1 μg/mL, which led to a reduction in the viability of HCC827 cells. (D) However, afatinib (10 ng/mL) clearly inhibited the formation of HCC827-derived tumorspheres by approximately 50% (n = 3), revealing that afatinib preferably inhibited cancer stemness. (E) Moreover, afatinib reduced EGFR autophosphorylation and expression and *Oct4* expression in the HCC827-derived tumorspheres, implying that EGFR phosphorylation self-regulated EGFR expression in HCC827 cells. Scale bar: 100 μm. $*p < 0.05$. $**p < 0.01$, $***p < 0.001$.

lung cancer, particularly for inhibiting EGFR phosphorylation by using gefitinib and afatinib. However, the mutations of EGFR-downstream proteins, such as KRAS in A549, result in drug resistance, protecting cancer cells from therapeutic treatments [18]. Moreover, the therapeutic inhibition of EGFR induces gene arrangement and acquired drug resistance against TKIs [30,31]. These drug resistance strategies include the induction of other oncogenic drivers, such as the induction of T790M mutations in the EGFR gene [32], MET [33], or HER2 amplifications [34]. Drug resistance is highly associated with CSC development [35,36]. The major downstream regulators determining cancer stemness are derived from either EGFR signaling or another drug-resistant pathway; therefore, they have been considered as therapeutic targets to overcome the acquired resistance from cancer stemness.

G9a, an SET domain-containing HMT, interacts with GLP to form heterodimers through the SET domain [37]. G9a-GLP methylates on H3K9 and H3K27 [38]. H3K9 methylation is considered to condense the genome chromatin and inhibit DNA transcription, thus indicating that G9a is a transcriptional corepressor. In addition to methylation on histones, G9a-GLP methylates nonhistone proteins [39]. G9a was revealed to activate p53 through a methylation-independent mechanism [40]. G9a was also reported to methylate p53 at Lys373, which is associated with p53 activity [39]. Additionally, a study revealed that G9a positively regulated gene expression by recruiting GRIP1, CARM1, and p300 [41]. Therefore, we speculate that G9a acts
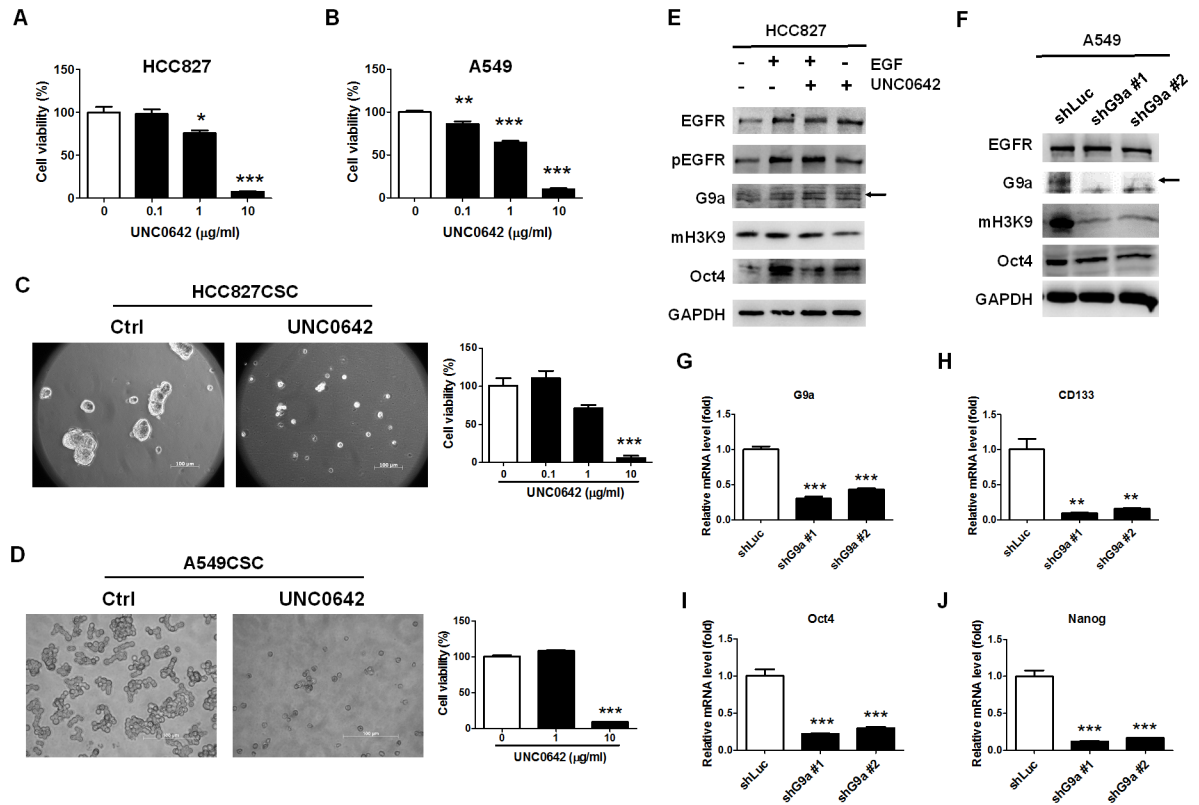
**Fig 4. G9a–GLP inhibitor, UNC0642, and G9a knockdown inhibited G9a-mediated H3K9 methylation and reduced stemness in lung cancer cells.** To determine that *G9a* is a regulator of stemness in lung cancer, the G9a–GLP inhibitor and genetic knockdown of G9a were applied to inhibit the formation of tumorspheres and expression of stemness markers, respectively. (A) We found that UNC0642 significantly reduced HCC827 cells when used at a dose of less than 1 μg/mL and (B) A549 cells when used at a dose of less than 0.1 μg/mL. (C) UNC0642 also significantly reduced the formation of HCC827 CSCs when used at a dose of 10 μg/mL and (D) A549 CSCs. The reduction in cell viability was similar to that observed for parental cells. (E) Therefore, to validate that the reduction in tumorsphere formation was derived from the inhibition of the cancer stemness property, *Oct4* was detected in UNC0642-treated HCC827 cells with or without 20 ng/mL of EGF. We found that UNC0642 reduced EGF-mediated mH3K9 and *Oct4* expression in HCC827 cells. (F) To validate the significant role of G9a in regulating the stemness property, we knocked down G9a by using shRNA technique and investigated the methylation of H3K9 and expression of *Oct4* in EGFR wild-type A549 cells. We found a marked reduction in H3K9 methylation and a slight reduction in *Oct4* expression in the *G9a* knockdown A549 cells. (G) The inhibition of *G9a* expression led to a reduction in the mRNA levels of (H) *CD133*, (J) *Oct4*, and (K) *Nanog*, indicating that *G9a* played a significant role in regulating the stemness property of lung cancer cells. Scale bar: 100 μm. *$p < 0.05$. **$p < 0.01$. ***$p < 0.001$.

as a coactivator under some cellular conditions instead of a gene repressor. However, the detailed mechanism of G9a in determining cancer stemness remains unclear. In this study, we found that *G9a* inhibition and knockdown by UNC0642 or an shRNA technique, respectively, reduced *Oct4* expression, implying that *G9a* induced *Oct4* expression as a co-activator. The results are not in concordance with the literature that *G9a*-induced methylation on H3K9 results in *Oct4* repression [42]. Since *Oct4* is an important transcriptional factor for regulating the pluripotency of embryonic stem cells [43], and *G9a* is essential for early embryogenesis [21]. Therefore, we believe that *G9a* overexpression in CSCs preferably positively regulates *Oct4* for the developmental transition of cancer stemness. However, the detailed mechanism of *G9a* in regulating cancer stemness warrants further investigation.

In their cohort study, Rada et al indicated *G9a* to be associated with a higher survival rate among patients with early lung cancer [40]. However, *G9a* was reported to be elevated and

associated with tumor invasion, leading to a poor survival rate among patients with lung cancer [44]. This result is in concordance with our findings based on the TCGA database in this study (Fig 2I). Notably, the status of CSCs is different from that of well-grown cancer cells; the cells are tolerant to treatments with slower growth capacity. Therefore, the artificial low attachment in serum-free medium mimics a stressful environment that enforces the cells to develop temporary stemness properties. *G9a* was demonstrated to be upregulated in many types of cancers [39] and is probably involved in the transition of stemness, thus resulting in a poor survival rate in clinical practice. A previous study revealed that *G9a* knockout could reduce embryonic cell growth in G9a$^{-/-}$ mutant mice [21], indicating that *G9a* is essential for early embryogenesis. In this study, we validated that cancer stemness, as measured using *Oct4* expression, was regulated by *G9a* in the temporary stemness status derived from EGFR-positive lung cancer cells, which was the EGFR-downstream protein serving as a therapeutic target.

We observed that 10 ng/mL of YM155 more significantly inhibited the formation of HCC827-derived CSCs than did afatinib and UNC0642. YM155, an imidazolium-based survivin-suppressing compound [10], binds and inhibits ILF3 [9]; this thus suggests that ILF3 may contribute to the EGFR-mediated stemness property in HCC827 cells. The detailed mechanism and function of ILF3 warrant investigation in the future. Studies have reported that YM155 can inhibit tumorsphere formation [6,45]. In addition, YM155 has many functions and inhibits at least EGFR and survivin, thus serving as an anti-tumor agent [5,6]. In this study, we observed that YM155 inhibited EGFR autophosphorylation and *G9a* expression, rendering it a potent agent against lung cancer stemness.

In conclusion, EGFR phosphorylation was high in HCC827- and A549-derived tumorspheres, and this phosphorylated EGFR positively regulated *G9a* expression. *G9a* activity was associated with *Oct4* expression, indicating that EGFR mediated the upregulation of *Oct4* through *G9a*. Moreover, we observed that inhibitors, namely YM155, afatinib, and UNC0642, efficiently reduced tumorsphere formation. YM155 had a stronger inhibitory capacity against cancer stemness by simultaneously inhibiting EGFR autophosphorylation and *G9a* expression. Our data strongly suggest that YM155 as an inhibitor of lung cancer stemness is a potent agent against lung cancer.

## Acknowledgments

## Author Contributions

**Conceptualization:** Jungshan Chang, Ai-Sheng Ho, Ken-Hong Lim, Chun-Chao Chang, Yi-Fang Chang, Cheng-Wen Wu.

**Data curation:** Chun-Chia Cheng, Chun-Chao Chang.

**Formal analysis:** Chun-Chia Cheng.

**Funding acquisition:** Huan-Chau Lin, Ai-Sheng Ho, Cheng-Wen Wu.

**Investigation:** Chun-Chia Cheng.

**Methodology:** Chun-Chia Cheng.

Project administration: Yi-Fang Chang, Cheng-Wen Wu.

Resources: Chun-Chao Chang.

Supervision: Ken-Hong Lim, Yi-Fang Chang, Cheng-Wen Wu.

Validation: Yu-Cheng Chang.

Writing – original draft: Chun-Chia Cheng.

Writing – review & editing: Stanley Ching-Cheng Huang, Ling Huang, Yi-Fang Chang, Cheng-Wen Wu.

# References

1. Arteaga CL, Engelman JA (2014) ERBB receptors: from oncogene discovery to basic science to mechanism-based cancer therapeutics. Cancer Cell 25: 282–303. https://doi.org/10.1016/j.ccr.2014.02.025 PMID: 24651011

2. Yarden Y, Pines G (2012) The ERBB network: at last, cancer therapy meets systems biology. Nat Rev Cancer 12: 553–563. https://doi.org/10.1038/nrc3309 PMID: 22785351

3. Lynch TJ, Bell DW, Sordella R, Gurubhagavatula S, Okimoto RA, Brannigan BW, et al. (2004) Activating mutations in the epidermal growth factor receptor underlying responsiveness of non-small-cell lung cancer to gefitinib. N Engl J Med 350: 2129–2139. https://doi.org/10.1056/NEJMoa040938 PMID: 15118073

4. Taus A, Vollmer I, Arriola E (2011) Activating and resistance mutations of the epidermal growth factor receptor (EGFR) gene and non-small cell lung cancer: a clinical reality. Arch Bronconeumol 47: 103–105. https://doi.org/10.1016/j.arbres.2010.06.013 PMID: 20678850

5. Na YS, Yang SJ, Kim SM, Jung KA, Moon JH, Shin JS, et al. (2012) YM155 induces EGFR suppression in pancreatic cancer cells. PLoS One 7: e38625. https://doi.org/10.1371/journal.pone.0038625 PMID: 22723871

6. Cheng XJ, Lin JC, Ding YF, Zhu L, Ye J, Tu SP (2016) Survivin inhibitor YM155 suppresses gastric cancer xenograft growth in mice without affecting normal tissues. Oncotarget 7: 7096–7109. https://doi.org/10.18632/oncotarget.6898 PMID: 26771139

7. Li Y, Rogoff HA, Keates S, Gao Y, Murikipudi S, Mikule K, et al. (2015) Suppression of cancer relapse and metastasis by inhibiting cancer stemness. Proc Natl Acad Sci U S A 112: 1839–1844. https://doi.org/10.1073/pnas.1424171112 PMID: 25605917

8. Zhang Y, Jin Z, Zhou H, Ou X, Xu Y, Li H, et al. (2016) Suppression of prostate cancer progression by cancer cell stemness inhibitor napabucasin. Cancer Med 5: 1251–1258. https://doi.org/10.1002/cam4.675 PMID: 26899963

9. Nakamura N, Yamauchi T, Hiramoto M, Yuri M, Naito M, Takeuchi M, et al. (2012) Interleukin enhancer-binding factor 3/NF110 is a target of YM155, a suppressant of survivin. Mol Cell Proteomics 11: M111 013243.

10. Nakahara T, Kita A, Yamanaka K, Mori M, Amino N, Takeuchi M, et al. (2007) YM155, a novel small-molecule survivin suppressant, induces regression of established human hormone-refractory prostate tumor xenografts. Cancer Res 67: 8014–8021. https://doi.org/10.1158/0008-5472.CAN-07-1343 PMID: 17804712

11. Hirsh V (2011) Afatinib (BIBW 2992) development in non-small-cell lung cancer. Future Oncol 7: 817–825. https://doi.org/10.2217/fon.11.62 PMID: 21732753

12. Ninomiya T, Takigawa N, Ichihara E, Ochi N, Murakami T, Honda Y, et al. (2013) Afatinib prolongs survival compared with gefitinib in an epidermal growth factor receptor-driven lung cancer model. Mol Cancer Ther 12: 589–597. https://doi.org/10.1158/1535-7163.MCT-12-0885 PMID: 23443806

13. Yu HA, Pao W (2013) Targeted therapies: Afatinib—new therapy option for EGFR-mutant lung cancer. Nat Rev Clin Oncol 10: 551–552. https://doi.org/10.1038/nrclinonc.2013.154 PMID: 23959269

14. Wang XK, He JH, Xu JH, Ye S, Wang F, Zhang H, et al. (2014) Afatinib enhances the efficacy of conventional chemotherapeutic agents by eradicating cancer stem-like cells. Cancer Res 74: 4431–4445. https://doi.org/10.1158/0008-5472.CAN-13-3553 PMID: 24972892

15. Sun FF, Hu YH, Xiong LP, Tu XY, Zhao JH, Chen SS, et al. (2015) Enhanced expression of stem cell markers and drug resistance in sphere-forming non-small cell lung cancer cells. Int J Clin Exp Pathol 8: 6287–6300. PMID: 26261505

16. Perona R, Lopez-Ayllon BD, de Castro Carpeno J, Belda-Iniesta C (2011) A role for cancer stem cells in drug resistance and metastasis in non-small-cell lung cancer. Clin Transl Oncol 13: 289–293. https://doi.org/10.1007/s12094-011-0656-3 PMID: 21596655

17. Liao HW, Hsu JM, Xia W, Wang HL, Wang YN, Chang WC, et al. (2015) PRMT1-mediated methylation of the EGF receptor regulates signaling and cetuximab response. J Clin Invest 125: 4529–4543. https://doi.org/10.1172/JCI82826 PMID: 26571401

18. Wang M, Kern AM, Hulskotter M, Greninger P, Singh A, Pan Y, et al. (2014) EGFR-mediated chromatin condensation protects KRAS-mutant cancer cells against ionizing radiation. Cancer Res 74: 2825–2834. https://doi.org/10.1158/0008-5472.CAN-13-3157 PMID: 24648348

19. Shankar SR, Bahirvani AG, Rao VK, Bharathy N, Ow JR, Taneja R (2013) G9a, a multipotent regulator of gene expression. Epigenetics 8: 16–22. https://doi.org/10.4161/epi.23331 PMID: 23257913

20. Purcell DJ, Khalid O, Ou CY, Little GH, Frenkel B, Baniwal SK, et al. (2012) Recruitment of coregulator G9a by Runx2 for selective enhancement or suppression of transcription. J Cell Biochem 113: 2406–2414. https://doi.org/10.1002/jcb.24114 PMID: 22389001

21. Tachibana M, Sugimoto K, Nozaki M, Ueda J, Ohta T, Ohki M, et al. (2002) G9a histone methyltransferase plays a dominant role in euchromatic histone H3 lysine 9 methylation and is essential for early embryogenesis. Genes Dev 16: 1779–1791. https://doi.org/10.1101/gad.989402 PMID: 12130538

22. Hsiao SM, Chen MW, Chen CA, Chien MH, Hua KT, Hsiao M, et al. (2015) The H3K9 Methyltransferase G9a Represses E-cadherin and is Associated with Myometrial Invasion in Endometrial Cancer. Ann Surg Oncol 22 Suppl 3: S1556–1565.

23. Liu S, Ye D, Guo W, Yu W, He Y, Hu J, et al. (2015) G9a is essential for EMT-mediated metastasis and maintenance of cancer stem cell-like characters in head and neck squamous cell carcinoma. Oncotarget 6: 6887–6901. https://doi.org/10.18632/oncotarget.3159 PMID: 25749385

24. Vlashi E, Kim K, Lagadec C, Donna LD, McDonald JT, Eghbali M, et al. (2009) In vivo imaging, tracking, and targeting of cancer stem cells. J Natl Cancer Inst 101: 350–359. https://doi.org/10.1093/jnci/djn509 PMID: 19244169

25. Reynolds BA, Tetzlaff W, Weiss S (1992) A multipotent EGF-responsive striatal embryonic progenitor cell produces neurons and astrocytes. J Neurosci 12: 4565–4574. PMID: 1432110

26. Shostak K, Chariot A (2015) EGFR and NF-kappaB: partners in cancer. Trends Mol Med 21: 385–393. https://doi.org/10.1016/j.molmed.2015.04.001 PMID: 25979753

27. Wang F, Wang S, Wang Z, Duan J, An T, Zhao J, et al. (2012) Phosphorylated EGFR expression may predict outcome of EGFR-TKIs therapy for the advanced NSCLC patients with wild-type EGFR. J Exp Clin Cancer Res 31: 65. https://doi.org/10.1186/1756-9966-31-65 PMID: 22901364

28. Quandt K, Frech K, Karas H, Wingender E, Werner T (1995) MatInd and MatInspector: new fast and versatile tools for detection of consensus matches in nucleotide sequence data. Nucleic Acids Res 23: 4878–4884. PMID: 8532532

29. Liu F, Barsyte-Lovejoy D, Li F, Xiong Y, Korboukh V, Huang XP, et al. (2013) Discovery of an in vivo chemical probe of the lysine methyltransferases G9a and GLP. J Med Chem 56: 8931–8942. https://doi.org/10.1021/jm401480r PMID: 24102134

30. Wu SG, Liu YN, Tsai MF, Chang YL, Yu CJ, Yang PC, et al. (2016) The mechanism of acquired resistance to irreversible EGFR tyrosine kinase inhibitor-afatinib in lung adenocarcinoma patients. Oncotarget 7: 12404–12413. https://doi.org/10.18632/oncotarget.7189 PMID: 26862733

31. Kim Y, Ko J, Cui Z, Abolhoda A, Ahn JS, Ou SH, et al. (2012) The EGFR T790M mutation in acquired resistance to an irreversible second-generation EGFR inhibitor. Mol Cancer Ther 11: 784–791. https://doi.org/10.1158/1535-7163.MCT-11-0750 PMID: 22228822

32. Kobayashi S, Boggon TJ, Dayaram T, Janne PA, Kocher O, Meyerson M, et al. (2005) EGFR mutation and resistance of non-small-cell lung cancer to gefitinib. N Engl J Med 352: 786–792. https://doi.org/10.1056/NEJMoa044238 PMID: 15728811

33. Engelman JA, Zejnullahu K, Mitsudomi T, Song Y, Hyland C, Park JO, et al. (2007) MET amplification leads to gefitinib resistance in lung cancer by activating ERBB3 signaling. Science 316: 1039–1043. https://doi.org/10.1126/science.1141478 PMID: 17463250

34. Takezawa K, Pirazzoli V, Arcila ME, Nebhan CA, Song X, de Stanchina E, et al. (2012) HER2 amplification: a potential mechanism of acquired resistance to EGFR inhibition in EGFR-mutant lung cancers that lack the second-site EGFRT790M mutation. Cancer Discov 2: 922–933. https://doi.org/10.1158/2159-8290.CD-12-0108 PMID: 22956644

35. Zhao M, Zhang Y, Zhang H, Wang S, Zhang M, Chen X, et al. (2015) Hypoxia-induced cell stemness leads to drug resistance and poor prognosis in lung adenocarcinoma. Lung Cancer 87: 98–106. https://doi.org/10.1016/j.lungcan.2014.11.017 PMID: 25512094

36. Dean M, Fojo T, Bates S (2005) Tumour stem cells and drug resistance. Nat Rev Cancer 5: 275–284. https://doi.org/10.1038/nrc1590 PMID: 15803154

37. Tachibana M, Ueda J, Fukuda M, Takeda N, Ohta T, Iwanari H, et al. (2005) Histone methyltransferases G9a and GLP form heteromeric complexes and are both crucial for methylation of euchromatin at H3-K9. Genes Dev 19: 815–826. https://doi.org/10.1101/gad.1284005 PMID: 15774718

38. Tachibana M, Sugimoto K, Fukushima T, Shinkai Y (2001) Set domain-containing protein, G9a, is a novel lysine-preferring mammalian histone methyltransferase with hyperactivity and specific selectivity to lysines 9 and 27 of histone H3. J Biol Chem 276: 25309–25317. https://doi.org/10.1074/jbc.M101914200 PMID: 11316813

39. Huang J, Dorsey J, Chuikov S, Perez-Burgos L, Zhang X, Jenuwein T, et al. (2010) G9a and Glp methylate lysine 373 in the tumor suppressor p53. J Biol Chem 285: 9636–9641. https://doi.org/10.1074/jbc.M109.062588 PMID: 20118233

40. Rada M, Vasileva E, Lezina L, Marouco D, Antonov AV, Macip S, et al. (2016) Human EHMT2/G9a activates p53 through methylation-independent mechanism. Oncogene.

41. Bittencourt D, Wu DY, Jeong KW, Gerke DS, Herviou L, Ianculescu I, et al. (2012) G9a functions as a molecular scaffold for assembly of transcriptional coactivators on a subset of glucocorticoid receptor target genes. Proc Natl Acad Sci U S A 109: 19673–19678. https://doi.org/10.1073/pnas.1211803109 PMID: 23151507

42. Kellner S, Kikyo N (2010) Transcriptional regulation of the Oct4 gene, a master gene for pluripotency. Histol Histopathol 25: 405–412. https://doi.org/10.14670/HH-25.405 PMID: 20054811

43. Nichols J, Zevnik B, Anastassiadis K, Niwa H, Klewe-Nebenius D, Chambers I, et al. (1998) Formation of pluripotent stem cells in the mammalian embryo depends on the POU transcription factor Oct4. Cell 95: 379–391. PMID: 9814708

44. Chen MW, Hua KT, Kao HJ, Chi CC, Wei LH, Johansson G, et al. (2010) H3K9 histone methyltransferase G9a promotes lung cancer invasion and metastasis by silencing the cell adhesion molecule Ep-CAM. Cancer Res 70: 7830–7840. https://doi.org/10.1158/0008-5472.CAN-10-0833 PMID: 20940408

45. Li L, Hao X, Qin J, Tang W, He F, Smith A, et al. (2014) Antibody against CD44s inhibits pancreatic tumor initiation and postradiation recurrence in mice. Gastroenterology 146: 1108–1118. https://doi.org/10.1053/j.gastro.2013.12.035 PMID: 24397969